Mechanical stress, fracture risk and beak evolution in Darwin's ground finches (*Geospiza*)

Joris Soons[1], Anthony Herrel[2,3,*], Annelies Genbrugge[1,4], Peter Aerts[3,5], Jeffrey Podos[6], Dominique Adriaens[4], Yoni de Witte[7], Patric Jacobs[8] and Joris Dirckx[1]

[1]*Laboratory of Biomedical Physics, University of Antwerp, Groenenborgerlaan 171, 2020 Antwerpen, Belgium*
[2]*Département d'Ecologie et de Gestion de la Biodiversité, Museum National d'Histoire Naturelle, 57 rue Cuvier, Case postale 55, 75231 Paris Cedex 5, France*
[3]*Department of Biology, University of Antwerp, Universiteitsplein 1, 2610 Antwerpen, Belgium*
[4]*Evolutionary Morphology of Vertebrates, Ghent University—UGent, K.L. Ledeganckstraat 35, 9000 Gent, Belgium*
[5]*Department of Movement and Sports Sciences, Ghent University, Watersportlaan 2, 9000 Gent, Belgium*
[6]*Department of Biology and Graduate Program in Organismic and Evolutionary Biology, University of Massachusetts, Amherst, MA 01003, USA*
[7]*Department of Subatomic and Radiation Physics, Ghent University—UGent, Proeftuinstraat 86, 9000 Gent, Belgium*
[8]*Department of Geology and Soil Science, University of Ghent, Krijgslaan 281/S8, 9000 Gent, Belgium*

Darwin's finches have radiated from a common ancestor into 14 descendent species, each specializing on distinct food resources and evolving divergent beak forms. Beak morphology in the ground finches (*Geospiza*) has been shown to evolve via natural selection in response to variation in food type, food availability and interspecific competition for food. From a mechanical perspective, however, beak size and shape are only indirectly related to birds' abilities to crack seeds, and beak form is hypothesized to evolve mainly under selection for fracture avoidance. Here, we test the fracture-avoidance hypothesis using finite-element modelling. We find that across species, mechanical loading is similar and approaches reported values of bone strength, thus suggesting pervasive selection on fracture avoidance. Additionally, deep and wide beaks are better suited for dissipating stress than are more elongate beaks when scaled to common sizes and loadings. Our results illustrate that deep and wide beaks in ground finches enable reduction of areas with high stress and peak stress magnitudes, allowing birds to crack hard seeds while limiting the risk of beak failure. These results may explain strong selection on beak depth and width in natural populations of Darwin's finches.

Keywords: Darwin's finches; finite-element modelling; bite force; beak shape

1. INTRODUCTION

Beak morphology in Darwin's finches has been shown to evolve via natural selection in response to variation in food type, food availability and interspecific competition for food (Lack 1947; Grant 1999; Grant & Grant 2006). Consequently, divergent beak sizes and shapes evolved in Darwin's finches specializing on different food items (Lack 1947; Bowman 1961; Grant 1999; Foster *et al.* 2008). Variation in beak shape in the ground finches of the genus *Geospiza* is situated mainly along two axes: variation in width and depth which covary, and variation in length (Bowman 1961). Species that crush hard seeds at the base of their beaks, such as *G. fortis* and *G. magnirostris*,

tend to have relatively short but wide and deep beaks (Grant 1999). Other species, such as *G. scandens* and *G. difficilis*, tend to have longer yet narrower and shallower beaks, a design that has been suggested to be a compromise between base crushing and probing (Bowman 1961). Interestingly, the two principal axes of variation observed within the ground finch clade are also reflected in distinct developmental pathways (Abzhanov *et al.* 2004, 2006).

While much research has focused on beak size and shape, the seed cracking ability of a bird is determined more directly by bite force capacity which is, in turn, closely dependent on jaw adductor muscle cross-sectional area (Bowman 1961; van der Meij & Bout 2004; Herrel *et al.* 2005a,b). The jaw closer muscles, situated at the back of the head, generate crushing forces that are transferred to food by means of the upper and lower beak (Herrel *et al.* 2005a,b). Beak morphology is thus expected to evolve in concert

Table 1. Calculated bite force, measured bite force and output of finite-element models.
(Bite forces calculated based on the morphology of the specimens and the finite-element model, bite forces measured in the field (10), and peak von Mises stress at three locations on the upper beak showing high stress concentrations (figure 1). von Mises stresses were calculated in two simulations; first, with the model loaded using the forces associated with each beak type (figure 2), and second when all beaks were scaled to the area of, and loaded with the forces of *G. fortis* (figure 3). Max. proc., maxillary process of the nasal bone (zone 2 in figure 1*a*); ipsilateral side, bite side (left); contralateral side, opposite side (right).)

species	scaled model volume (mm^3)	calculated bite force (N)	measured bite force (N)	peak von Mises' stress real loading (MPa)			peak von Mises' stress *G. fortis* loading (MPa)		
				dorsal nasal	ipsilateral max. proc.	contralateral max. proc.	dorsal nasal	ipsilateral max. proc.	contralateral max. proc.
G. fortis	112	28.5	26.6 ± 6.5	31.0	41.0	42.0			
G. fuliginosa	120	5.6	4.7 ± 1.5	19.8	24.2	25.2	30.2	35.9	38.7
G. scandens	108	8.4	7.2 ± 1.6	32.9	44.6	32.9	42.6	50.8	61.2
G. magnirostris	89						35.3	42.9	43.9
G. difficilis	66						53.6	49.7	71.5

with jaw adductor force generation capacity, through selection for the capacity to avoid structural failure under conditions of increased muscle and food reaction forces (Bowman 1961). Indeed, almost 50 years ago, Bowman (1961) suggested that the shape of the beak was adapted for fracture resistance, with beaks with more or less straightened culmen or gonys (upper and lower beak, respectively) tending to reduce fracture risk. Modifications towards increased beak depth, on the other hand, were interpreted as adaptations towards more powerful crushing bites (Bowman 1961).

To test these hypotheses, we developed finite-element models (FEMs) of the upper beak in ground finches (table 1). As FEMs quantify the effect of complex shape variation on stress magnitude and distribution (Richmond *et al.* 2005; Ross 2005; Rayfield 2007; Rayfield & Milner 2008), they are ideally suited to address the hypothesis that beak shape has evolved in response to fracture avoidance, and may also offer insights into observed patterns of selection on beak shape (depth, width and curvature) in species that crack hard seeds.

2. MATERIAL AND METHODS

(a) *Fresh specimens and muscle data*
Road-killed specimens were collected during February–March of 2005 and 2006 on Santa Cruz Island, under a salvage permit from the Galápagos National Park Service. Intact specimens were collected and preserved in a 10 per cent aqueous formaldehyde solution for 24 h, rinsed and transferred to a 70 per cent aqueous ethanol solution. Specimens were transported to Belgium where one individual each of *G. fortis*, *G. fuliginosa* and *G. scandens* was scanned at the Centre for X-ray Tomography, Ghent University (UGCT) scanning facility. A second specimen of each of these species was dissected and all jaw muscle bundles were removed individually. Muscles were blotted dry and weighed on a Mettler microbalance (± 0.01 mg). Next, muscles were transferred individually to Petri dishes and submerged in a 30 per cent aqueous nitric acid solution for 18 h to dissolve all connective tissue (Loeb & Gans 1986).

After removal of nitric acid, muscles were transferred to a 50 per cent aqueous glycerol solution and fibres teased apart using blunt-tipped glass needles. Next, 30 fibres were selected and drawn using a binocular scope with attached camera lucida. A background grid was also drawn in each image to provide an object for scaling. Drawings were scanned and fibre lengths determined using Scion Image (freely available at http://www.scioncorp.com).

Based on the muscle mass and fibre lengths, the physiological cross-sectional area of each muscle bundle was determined assuming a muscle density of 1060 kg m^{-3} (Méndez & Keys 1960). As pennate muscles were separated into their individual bundles, no additional correction for pennation angle was included. Force generation capacity for each muscle was calculated assuming a muscle stress of 30 N cm^{-2} (Nigg & Herzog 1999). As the external adductor and pseudotemporalis muscle bundles act only indirectly on the upper beak through the jugal bone (Nuijens & Zweers 1997; van der Meij & Bout 2004), the component of the muscle force transferred to the upper beak was calculated by taking into account the position of the muscles and the angle thereof relative to the jugal bone. The pterygoid muscle bundles, by contrast, act directly on the upper beak (Nuijens & Zweers 1997; van der Meij & Bout 2004) and muscle forces were assumed to be directly transmitted through the pterygoid–palatine complex.

(b) *CT scanning and reconstruction*
Road-killed specimens of *G. fortis*, *G. fuliginosa* and *G. scandens* were scanned at the UGCT scanning facility (www.ugct.ugent.be), using a micro-focus directional type X-ray tube, set at a voltage of 80 kVp and a spot size of 10 µm. Specimens were mounted on a controllable rotating table (MICOS, UPR160F-AIR). For each specimen, a series of 1000 projections of 940×748 pixels were recorded covering $360°$ resulting in voxel sizes of 43.73 µm for *G. fortis*, 34.84 µm for *G. fuliginosa* and 42.77 µm for *G. scandens*. Reconstruction of the tomographic projection data was done using the OCTOPUS package (Vlassenbroeck *et al.* 2007).

Specimens of *G. difficilis* (MCZ39828) and *G. magnirostris* (MCZ65745) were scanned at the Harvard CNS facility using an X-Tek XRA-002 micro-CT imaging system set at 75 kV. Specimens were mounted on a rotating table and a series of 3142 projections of 2000 by 2000 pixels covering 360° was recorded resulting in voxel sizes of 25.26 μm for *G. difficilis* and 45.75 μm for *G. magnirostris*. Reconstruction of the tomographic projections was done using CTPro (Metris) and VGStudio Max 2.0 (Volume Graphics). Volume and surface rendering was performed using Amira 5.0 (64-bit version, Computer Systems Mercury) for all specimens.

(c) Finite-element modelling

CT-image sequences were segmented semi-automatically based on greyscale thresholding and smoothed using Amira 5.0 (64-bit version, Computer Systems Mercury), to obtain a triangular surface mesh of the upper beak (figure 1). Next, a Delaunay tetrahedral volume mesh with a minimum radius: edge ratio of 1.4 was generated in TetGen (Si 2008) and imported in the finite-element program FEBio (Maas & Weiss 2008). A left unilateral load with all muscles bilaterally activated to 100 per cent was applied at a posterior bite point, the position of which was determined based on recordings of birds cracking seeds in the field. For each modelled specimen, the bite point was simulated through a translation constraint of the corresponding elements. The fronto-nasal hinge was modelled as two rotating but fixed elements. The forces on palatine and jugal bones were applied along the long axis of these bones as determined on the CT data, and with a magnitude derived from calculated muscle forces. Bone was modelled as a linear elastic, isotropic and homogeneous material with Young's modulus of 18 GPa, and a Poisson ratio of 0.3 (Yamada 1970; Evans 1973; Vogel 2003; Currey 2006). Linear elements were used in the models, which were solved with an iterative Newton-based Broyden–Fletcher–Goldfarb–Shanno (BFGS) solver. The convergence and the stability of the results were tested by an iterative refinement of the mesh up to 500 000 elements and terminated at an accuracy of 5 per cent or better.

As stress is a complex three-dimensional phenomenon, inherently difficult to interpret, we chose to combine the stresses using the von Mises criterion. Three areas with high stress were noted in our simulations: posterior on the maxilla in front of the nasal apertures, and on the ipsi- and contralateral processi maxillari of the nasal bone. A high stress area posterior on the beak was not considered because high stresses in this region may be due to constraints imposed at the fronto-nasal hinge. The maximal von Mises stress observed in a volume with a predefined radius was recorded in all areas showing high stress, and compared across loading conditions for the different species (table 1). Peak stress values were recorded in meshes of increasing complexity allowing us to test the convergence of the model solution (Herrel *et al.* in press). Additionally, the external force needed to satisfy the constraint at the bite point, perpendicular
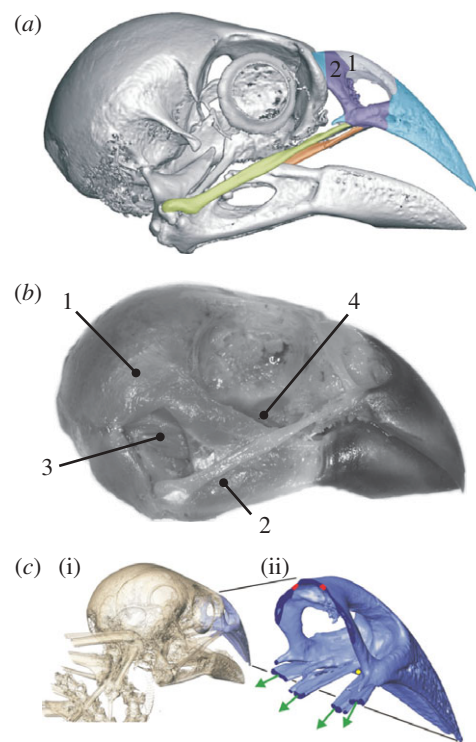
to the surface area, was calculated and the magnitude thereof was recorded and compared with the bite forces measured *in vivo* (table 1). Finally, FE models for *G. difficilis*, *G. fuliginosa*, *G. magnirostris* and *G. scandens* were scaled by model area (Dumont *et al.* 2009) to the same size as the *G. fortis* model, and simulations were run with input forces based on *G. fortis* in order to evaluate how beak shape affects loading of the beak.

Figure 1. Schematic overview of the model derivation and methods. (*a*) Lateral view of a three-dimensional reconstruction of the skull of a medium ground finch (*G. fortis*) based on micro-CT scans. When birds bite, forces are transmitted by the jaw muscles to the upper beak (blue) via the jugal bones (green) and the pterygoid–palatine complex (orange). The coloured zone labelled 1 represents the dorsal nasal region, and the zone labelled 2 represents the maxillary process of the nasal bone. (*b*) Photograph of the head of a *G. fortis* specimen, skin removed, illustrating the major jaw closing muscles. The external adductor muscles (1, 2) and the m. pseudotemporalis (3) transmit force to the upper beak through the jugal bone. The pterygoideus muscles (4) directly pull the upper beak downward through the pterygoid–palatine complex. (*c*) Posterior oblique view of (i) the head and (ii) upper beak of a *G. fortis*, illustrating loadings and constraints used in the finite-element models. Red zones indicate the dorsal constraints on the rotating fixed elements, (i) the yellow circle indicates the bite point and green arrows indicate the orientation of the load acting on the jugals and palatines.

3. RESULTS

The three species of Darwin's finch featured in our analysis showed a nearly threefold absolute difference in the cross-sectional area of the jaw adductor muscles (0.28 mm² in *G. fuliginosa* versus 0.72 mm² in *G. fortis*), and thus also in the maximal potential loading of the beak. A first set of FEM simulations was performed using actual beak size and shape as
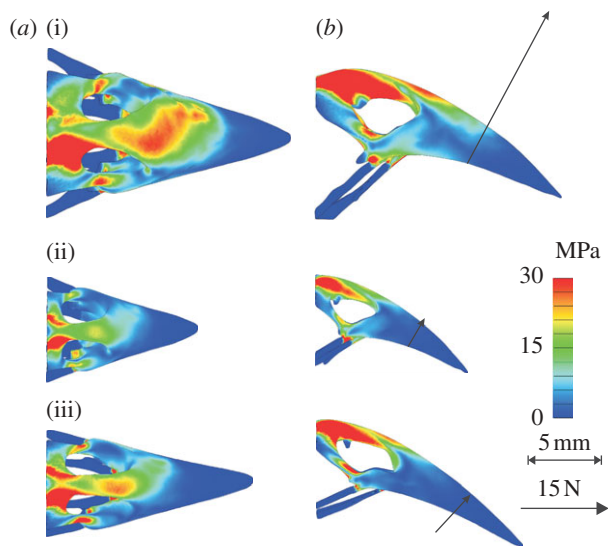
Figure 2. Output of finite-element analyses performed for three different species of ground finches (*Geospiza*) for which specimens were available for dissection. Input forces were calculated from muscle mass and fibre length measurements. Colours indicate calculated resultant von Mises stresses on the beak in (*a*) dorsal and (*b*) lateral views: (i) *G. fortis*, (ii) *G. fuliginosa*, and (iii) *G. scandens*. Warmer colours depict higher stresses. For all species, maximum stress concentration occurs at the posterior part of the nasal bone, posterior to the nasal aperture (zone 1 in figure 1*a*), and within the maxillary processes of the nasal bone (zone 2 in figure 1*a*). Arrows depict calculated bite forces.

determined from CT scans, and applied input forces based on information derived from muscle dissections for the three species for which specimens were available for dissection. Results from these simulations show that beaks in all species show stress concentrations in similar regions, specifically in the region of the nasal bone posterior to the nasal aperture, and in the processi maxillari of the nasal bone (figure 2). Stresses were typically highest at the dorsal and posterior aspect of the nasal bone and at the processus maxillaris contralateral to the bite side (figure 2 and table 1).

A second set of FEM simulations was performed in which beaks were scaled to the area of the *G. fortis* specimen, and then loaded using the input forces calculated for this species (figure 3). This was done to characterize the potential effects of beak shape variation on force dissipation. If interspecific variation in beak shape does not impact force dissipation, all simulations would show comparable stress distributions and stress magnitudes. In contrast, the results identify marked differences among species in stress distributions, thus demonstrating the importance of beak shape in force dissipation. Species with elongate beaks such as *G. scandens* and *G. difficilis* show notable increases in the surface area subjected to high stress, spreading forward to the dorsal aspect, anterior of the nasal aperture. Moreover, the peak stresses calculated for the species with the longer and narrower beaks (*G. scandens* and *G. difficilis*; table 1) were substantially higher (maximum of 72 MPa). In contrast, the tall and wide beaks as seen in *G. fortis*, *G. fuliginosa* and *G. magnirostris* are seen to distribute the load
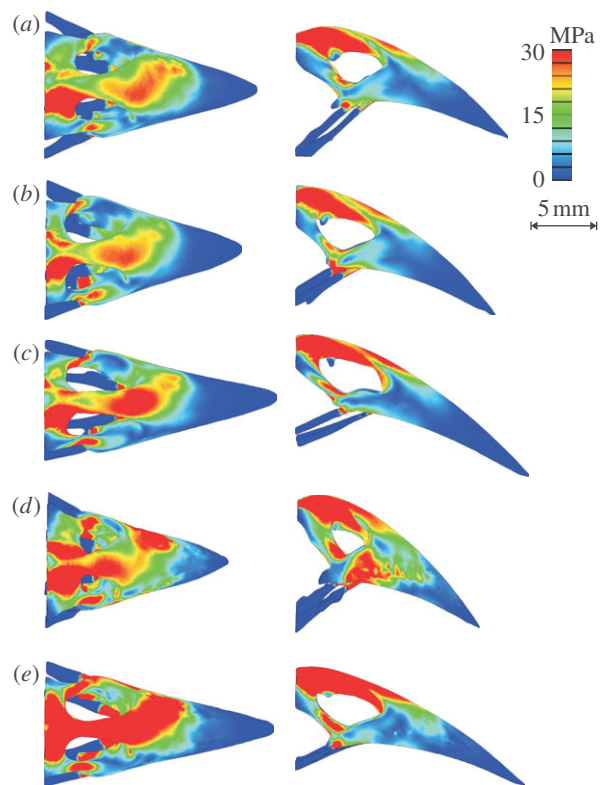

Figure 3. Output of a finite-element simulation, in which beak surface area of the five species of ground finch was scaled to a common surface area (that of *G. fortis*) prior to calculations, and in which the input force calculated for *G. fortis* was applied to all species. This simulation enables the evaluation of the effects of beak shape on stress distribution. The relatively long and slender beaked *G. scandens* and *G. difficilis* showed disproportional increases in the magnitude of the von Mises stress and the distribution of areas with high stress (table 1). (*a*) *G. fortis*, (*b*) *G. fuliginosa*, (*c*) *G. scandens*, (*d*) *G. magnirostris*, and (*e*) *G. difficilis*.

applied to the beak with lower peak stress values (maximum of 44 MPa across the three species), largely confined to the posterior aspect of the nasal bone. Note, however, how an additional area of high stress in the *G. magnirostris* model is present at the level of the bite point.

4. DISCUSSION

A comparison of the bite forces calculated in our FEMs with actual bite forces measured *in vivo* (table 1) shows that calculated values fall within the *in vivo* range, thus confirming that our models provide realistic estimates of beak loadings. Interestingly, our results provide one of the few cases where the output of FEMs is validated against *in vivo* data and suggest that FEMs can provide realistic output if based on realistic inputs (see Rayfield 2007 for an overview; Kupczik *et al*. 2009; Strait *et al*. 2009). However, our models must be considered as only a first step, and planned future models including the keratinous rhamphotheca and material properties for the beaks of Darwin's finches are needed to test whether a refinement of our models affects the output of our FE models in terms of stress distributions and magnitudes. Additionally, analyses of how constraints and

loading conditions affect stress magnitudes and distributions in beaks with different morphologies are needed and currently underway (Herrel *et al.* in press).

A comparison of peak stresses reported here in the different species of Darwin's finch with values reported for the compressive strength of bone suggests that Darwin's finch beaks operate with safety factors of between 3 and 5 in most species, assuming an average compressive bone strength of 165 MPa (note that bone strength ranges from 106 to 224 MPa across a wide range of vertebrates; Yamada 1970; Vogel 2003; Currey 2006). However, it should be noted that these are conservative estimates of safety factors as bone is known to fail in tension at much lower stresses (e.g. 117 MPa; Evans 1973). However, without specific data on material properties for the beaks of the birds considered here, this must remain speculative to some degree. Moreover, von Mises stress is often considered to be one of the best predictors of bone failure (Keyak & Rossi 2000), making it an appropriate value to use in the calculation of safety factors. Previously, it was suggested that beak morphology should evolve in concert with the force generating capacity of the jaw adductors through selection for the capacity to avoid structural failure under conditions of increased muscle and food reaction forces (Bowman 1961). Our data support this assertion and suggest that beaks are indeed optimized to withstand their natural loading regimes.

Almost five decades ago, Bowman (1961) suggested that the shape of the beak in Darwin's finches was related to fracture resistance, such that beaks with a more or less straightened culmen and gonys (the upper and lower beak, respectively) tend to reduce fracture risk. Modifications towards increased beak depth, on the other hand, were interpreted as adaptations towards a more powerful crushing bite (Bowman 1961). Our data provide only partial support for these hypotheses. Whereas deeper and wider beaks indeed appear better suited to withstand reaction forces from biting and may thus allow for higher bite forces, the straighter beaks of *G. scandens* and *G. difficilis* clearly induce greater stresses, thus presumably increasing fracture risk. The difference between *G. difficilis* and *G. fuliginosa* is especially notable, with the highest peak von Mises stress in *G. difficilis* being almost twice that of *G. fuliginosa* when scaled to the same surface area. Interestingly, however, the beak with the greatest curvature in *G. magnirostris* is seen to perform somewhat more poorly than that of *G. fuliginosa* when scaled to the same surface area, suggesting that too much curvature may negatively affect stress magnitudes as predicted by Bowman (1961). Alternatively, the relatively high stress may be due to the relatively low volume (and thus bone present) of the upper beak of the *G. magnirostris* specimen used in our models (see table 1). As this specimen and the *G. difficilis* used are dried historical specimens, this may represent a preservation artefact, and thus results for both *G. difficilis* and *G. magnirostris* should be interpreted with caution. Testing for potential preservation artefacts will require freshly preserved specimens, which may prove to be difficult to obtain.

In summary, our results illustrate that deep and wide beaks in Darwin's finches, long associated with

an ability to crack hard seeds, more specifically limit beak areas that experience high stress and peak stress magnitudes. Consequently, deep and wide beaks may allow birds to crack hard seeds while limiting the risk of beak failure. Deeper beaks are indicative of deeper dorsal nasal regions, and wider beaks indicative of a broader maxillary process of the nasal bone, the two areas typically showing high stress concentrations in our model. Thus, our simulations may help explain the low survival of birds with smaller beaks in times of food scarcity when seeds of intermediate size are rapidly depleted from the environment (Boag & Grant 1981). Given the often large within-population variation in beak size and shape (Grant 1983, 1999; Grant & Grant 2006), birds with relatively smaller (more narrow or shallow) beaks for a given jaw adductor size may be subject to mechanical failure more rapidly under the repeated loading needed to crack hard seeds such as *Tribulus* (Grant 1981) which are relatively abundant during dry years (Grant 1999). Finally, our data show how jaw musculature and beak shape have coevolved in Darwin's finches that specialize on different food resources. We suggest that finch jaw musculature and its relationship to beak safety factors is as critical in finch evolution and adaptive radiation as is the evolution of beak morphology itself. Future modelling efforts, including other radiations of birds specializing on cracking seeds, will be crucial to test the generality of our results.

REFERENCES

Abzhanov, A., Protas, M., Grant, R. B., Grant, P. R. & Tabin, C. J. 2004 Bmp4 and morphological variation of beaks in Darwin's finches. *Science* **305**, 1462–1465. (doi:10.1126/science.1098095)

Abzhanov, A., Kuo, W. P., Hartmann, C., Grant, B. R., Grant, P. R. & Tabin, C. J. 2006 The calmodulin pathway and evolution of elongated beak morphology in Darwin's finches. *Nature* **442**, 563–567. (doi:10.1038/nature 04843)

Boag, P. T. & Grant, P. R. 1981 Intense natural selection in a population of Darwin's finches (Geospizinae) in the Galapagos. *Science* **214**, 82–85. (doi:10.1126/science. 214.4516.82)

Bowman, R. I. 1961 Morphological differentiation and adaptation in the Galapagos finches. *Univ. Calif. Publ. Zool.* **58**, 1–302.

Currey, J. D. 2006 *Bones: structure and mechanics*. Princeton, NJ: Princeton University Press.

Dumont, E. R., Grosse, I. R. & Slater, G. J. 2009 Requirements for comparing the performance of finite element models of biological structures. *J. Theor. Biol.* **256**, 96–103. (doi:10.1016/j.jtbi.2008.08.017)

Evans, F. G. 1973 *Mechanical properties of bone*. Springfield, MA: Charles C. Thomas.

Foster, D., Podos, J. & Hendry, A. P. 2008 A geometric morphometric appraisal of beak shape in Darwin's finches. *J. Evol. Biol.* **21**, 263–275.

Grant, P. R. 1981 The feeding of Darwin's finches on *Tribulus cistoides* (L.) seeds. *Anim. Behav.* **29**, 785–793. (doi:10.1016/S0003-3472(81)80012-7)

Grant, P. R. 1983 Inheritance of size and shape in a population of Darwin's finches, *Geospiza conirostris*. *Proc. R. Soc. B* **220**, 219–236. (doi:10.1098/rspb.1983.0096)

Grant, P. R. 1999 *The ecology and evolution of Darwin's finches*. Princeton, NJ: Princeton University Press.

Grant, P. R. & Grant, B. R. 2006 Evolution of character displacement in Darwin's finches. *Science* **313**, 224–226. (doi:10.1126/science.1128374)

Herrel, A., Podos, J., Huber, S. K. & Hendry, A. P. 2005*a* Evolution of bite force in Darwin's finches: a key role for head width. *J. Evol. Biol.* **18**, 669–675. (doi:10.1111/j.1420-9101.2004.00857.x)

Herrel, A., Podos, J., Huber, S. K. & Hendry, A. P. 2005*b* Bite performance and morphology in a population of Darwin's finches: implications for the evolution of beak shape. *Funct. Ecol.* **19**, 43–48. (doi:10.1111/j.0269-8463.2005.00923.x)

Herrel, A., Soons, J., Aerts, P., Dirckx, J., Boone, M., Jacobs, P., Adriaens, D. & Podos, J. In press. Adaptation and function of Darwin's finch beaks: divergence by feeding type and sex. *Emu*.

Keyak, J. H. & Rossi, S. A. 2000 Prediction of femoral fracture load using finite element models: an examination of stress- and strain-based failure models. *J. Biomech.* **33**, 209–214. (doi:10.1016/S0021-9290(99)00152-9)

Kupczik, K., Dobson, C., Phillips, R., Oxnard, C., Fagan, M. & O'Higgins, P. 2009 Masticatory loading and bone adaptation in the supraorbital torus of developing macaques. *Am. J. Phys. Anthropol.* **139**, 193–203. (doi:10.1002/ajpa.20972)

Lack, D. 1947 *Darwin's finches*. Cambridge, UK: Cambridge University Press.

Loeb, G. E. & Gans, C. 1986 *Electromyography for experimentalists*. Chicago, IL: University of Chicago Press.

Maas, S. & Weiss, J. A. 2008 FEBio: finite elements for biomechanics. User's manual, v. 1.0. See http://mrl.sci.utah.edu/uploads/FEBio_um.pdf.

Méndez, J. & Keys, A. 1960 Density and composition of mammalian muscle. *Metabolism* **9**, 184–188.

Nigg, B. M. & Herzog, W. 1999 *Biomechanics of the musculo-skeletal system*. New York, NY: Wiley.

Nuijens, F. W. & Zweers, G. A. 1997 Characters discriminating two seed husking mechanisms in finches (Fringillidae: Carduelinae) and estrildids (Passeridae: Estrildinae). *J. Morphol.* **232**, 1–33. (doi:10.1002/(SICI)1097-4687(199704)232:1<1::AID-JMOR1>3.0.CO;2-G)

Rayfield, E. J. 2007 Finite element analysis and understanding the biomechanics and evolution of living and fossil organisms. *Annu. Rev. Earth Planet. Sci.* **35**, 541–576. (doi:10.1146/annurev.earth.35.031306.140104)

Rayfield, E. J. & Milner, A. C. 2008 Establishing a framework for archosaur cranial mechanics. *Paleobiology* **34**, 494–515. (doi:10.1666/07006.1)

Richmond, B. G., Wright, B. W., Grosse, I., Dechow, P. C., Ross, C. F., Spencer, M. A. & Strait, D. S. 2005 Finite-element analysis in functional morphology. *Anat. Rec.* **283A**, 259–274. (doi:10.1002/ar.20169)

Ross, C. F. 2005 Finite-element modeling in vertebrate biomechanics. *Anat. Rec.* **283A**, 253–258. (doi:10.1002/ar.a.20177)

Si, H. 2008 TetGen: a quality tetrahedral mesh generator and three-dimensional Delaunay triangulator. See http://tetgen.berlios.de.

Strait, D. S. *et al.* 2009 The feeding biomechanics and dietary ecology of *Australopithecus africanus*. *Proc. Natl Acad. Sci. USA* **106**, 2124–2129. (doi:10.1073/pnas.0808730106)

van der Meij, M. A. A. & Bout, R. G. 2004 Scaling of jaw muscle size and maximal bite force in finches. *J. Exp. Biol.* **207**, 2745–2753. (doi:10.1242/jeb.01091)

Vlassenbroeck, J., Dierick, M., Masschaele, B., Cnudde, V., van Hoorebeke, L. & Jacobs, P. 2007 Software tools for quantification of X-ray microtomography at the UGCT. *Nucl. Inst. Meth. Phys. Res. A* **580**, 442–445. (doi:10.1016/j.nima.2007.05.073)

Vogel, S. 2003 *Comparative biomechanics: life's physical world*. Princeton, NJ: Princeton University Press.

Yamada, H. 1970 *Strength of biological materials*. Baltimore, MD: Williams and Wilkins.